

Optimizing $pp \rightarrow A \rightarrow Z^* h \rightarrow \ell^+ \ell^- b \bar{b}$ Searches at the LHC in the 2HDM Type-I with Inverted Hierarchy

A.G. Akeroyd,^{1,*} S. Alanazi,^{1,2,†} and S. Moretti^{1,3,‡}

¹*School of Physics and Astronomy,
University of Southampton, Highfield,
Southampton SO17 1BJ, United Kingdom*

²*Physics Department, Imam Mohammad Ibn Saud Islamic University (IMISU),
P.O. Box 90950, Riyadh, 11623, Saudi Arabia*

³*Department of Physics and Astronomy,
Uppsala University, Box 516, 751 20 Uppsala, Sweden*

Abstract

In this study, we investigate the Large Hadron Collider (LHC) search for the signal process $pp \rightarrow A \rightarrow Z^* h \rightarrow \ell^+ \ell^- b \bar{b}$ ($\ell = e, \mu$) within the framework of the 2-Higgs-Doublet Model (2HDM) Type-I, considering an Inverted Hierarchy (IH) scenario wherein the Standard Model (SM)-like Higgs boson H is heavier than h (i.e., $m_h < m_H = 125$ GeV). We reproduce the dominant background distributions from a CMS analysis of $pp \rightarrow H \rightarrow ZA \rightarrow \ell^+ \ell^- b \bar{b}$ (for a on-shell Z), which we do for validation purposes, so that we can explore different invariant mass selection criteria to enhance the signal significance of our target process. Specifically, we compare the CMS baseline cuts ($70 \text{ GeV} < m_{\ell^+ \ell^-} < 110 \text{ GeV}$, no $m_{b \bar{b}}$ restriction) with the alternative selections $20 \text{ GeV} < m_{\ell^+ \ell^-} < 50 \text{ GeV}$ with $m_{b \bar{b}} < 100 \text{ GeV}$. The latter cuts are enforced to account for the off-shellness of the Z^* boson and the low mass Higgs state in our case. We show that these modifications reduce drastically the dominant Drell-Yan (DY) and top-(anti)quark pair backgrounds, leading to a significant excess from the analysis of the reconstructed $m_{\ell^+ \ell^- b \bar{b}}$ invariant mass in the illustrative ranges $145 \text{ GeV} < m_A < 150 \text{ GeV}$ and $68 \text{ GeV} < m_h < 75 \text{ GeV}$. Our results demonstrate that such cuts enable effective signal discrimination, suggesting an optimized strategy in future searches for an established topology but in a new kinematical regime, which is of particular relevance to the 2HDM Type-I with IH in its mass spectrum.

*Electronic address: a.g.akeroyd@soton.ac.uk

†Electronic address: swa1a19@soton.ac.uk; SWAlanazi@imamu.edu.sa

‡Electronic address: stefano.moretti@cern.ch

I. INTRODUCTION

The discovery of a Higgs boson in 2012 at the LHC marked a significant milestone in particle physics, yet the possibility of an extended Higgs sector remains an open question. One well-motivated extension of the SM is the 2HDM, which introduces several (pseudo)scalar Higgs states: two charged ones H^\pm , one CP-odd one A and two CP-even ones h and H (with, conventionally, $m_h < m_H$). Because h and H have zero electric charge and exhibit the same parity, this opens the door for a scenario where one of these two states matches the discovered one. To control Flavor-Changing Neutral Currents (FCNCs), a discrete \mathbb{Z}_2 symmetry is customarily applied to the 2HDM. This leads to four so-called Yukawa types of it: Type-I, -II, -Flipped and -Lepton Specific, depending on how this symmetry is assigned to the fermions and Higgs doublets [1].

In this theoretical context, we explore the IH scenario, wherein the heavier CP-even neutral Higgs boson H corresponds to the discovered Higgs state, in the 2HDM Type-I (i.e., $m_H = 125$ GeV). Under this condition, the production and decay mode $pp \rightarrow A \rightarrow Z^{(*)}h$ provides an interesting channel for probing such a new physics, where the weak gauge boson can be either on- (Z) or off-shell (Z^*). A possible final state emerging from this process is $\ell^+\ell^-b\bar{b}$, due to further $Z^{(*)}$ and h decays, respectively, which has been studied in several phenomenological and experimental papers. However, in the spirit of Ref. [2], and based on Ref. [3], which studied the processes $pp \rightarrow H \rightarrow ZA$ and $pp \rightarrow A \rightarrow ZH$ in the $\ell^+\ell^-b\bar{b}$ final state at $\sqrt{s} = 13$ TeV with 35.9 fb^{-1} of CMS data, we replicated the dominant background contributions (DY and $t\bar{t}$) from that analysis. This places us in the position of addressing the possibility of extracting our target signal in the complementary mode $pp \rightarrow A \rightarrow Z^{(*)}h$, i.e., with $m_A < 215$ GeV.

Therefore, in this short letter, based on previous results of ours on the signal [4–6]*, we investigate the process $pp \rightarrow A \rightarrow Z^*h \rightarrow \ell^+\ell^-b\bar{b}$ and explore optimized selection criteria that enhance its significance. We consider the two aforementioned main backgrounds, DY ($q\bar{q} \rightarrow \gamma^*, Z \rightarrow \ell^+\ell^-$) and top-(anti)quark pair production ($gg, q\bar{q} \rightarrow t\bar{t}$ with two leptonic decays of the emerging W^\pm pair). By comparing different invariant mass selection criteria, we demonstrate that specific mass cuts can significantly suppress such backgrounds while

* We note that a similar study to ours (chiefly, exploiting the off-shellness of the Z^* boson) was already carried out in Ref. [7], albeit for a 2HDM Type-II wherein h was the SM-like Higgs boson.

retaining the majority of signal events, ultimately improving the LHC sensitivity to the $pp \rightarrow A \rightarrow Z^* h$ channel in the 2HDM Type-I scenario with IH, crucially, for the case of an off-shell Z^* .

Experimental searches for new Higgs bosons in the $\ell^+ \ell^- b \bar{b}$ final state have mainly targeted the process $pp \rightarrow A \rightarrow Z h_{\text{SM}}$, under the assumption that the lighter CP-even state h of the 2HDM is the observed 125 GeV Higgs boson h_{SM} (standard mass hierarchy) and that the Z is produced on-shell. Specifically, the CMS search at 13 TeV with 35.9 fb $^{-1}$ of Ref. [8] probed the mass range $m_A = 225\text{--}1000$ GeV while the corresponding ATLAS analyses at 8 TeV with 20.3 fb $^{-1}$ [9] and 13 TeV with 139 fb $^{-1}$ [10] explored the range $m_A = 220\text{--}800$ GeV. By contrast, Ref. [3] studied the related processes $pp \rightarrow H \rightarrow ZA$ and $pp \rightarrow A \rightarrow ZH$ in the same final state, using the 2016 CMS dataset at 13 TeV with 35.9 fb $^{-1}$. In this case the two additional neutral Higgs bosons (i.e., non-SM-like) of the 2HDM were searched for in the ranges $120 \text{ GeV} < m_H < 1000 \text{ GeV}$ and $30 \text{ GeV} < m_A < 1000 \text{ GeV}$, respectively. The last analysis is particularly relevant to our work because it also allows for the IH interpretation when the heavier CP-even state of the 2HDM plays the role of the discovered 125 GeV Higgs. However, the mass range explored in Ref. [3] implies that the Z boson is always on-shell (i.e., $m_A > m_Z + m_H$ in the $pp \rightarrow A \rightarrow ZH$ channel).

The plan of the paper is as follows. In the next section, we describe our methodology. We then move on to present our results before concluding in the last section.

II. METHODOLOGY

This section provides an overview of the two largest backgrounds to the signal process $pp \rightarrow A \rightarrow Z^* h \rightarrow \ell^+ \ell^- b \bar{b}$, which are DY and top-(anti)quark pair production. The search in [3] is carried out with LHC Run 2 pp collision data corresponding to an integrated luminosity of 35.9 fb $^{-1}$, which was collected by the CMS experiment. We computed the signal $pp \rightarrow A \rightarrow Z^* h \rightarrow \ell^+ \ell^- b \bar{b}$ for two Benchmark Points (BPs) within the framework of the 2HDM Type-I, considering the IH scenario with $m_H = 125$ GeV, $m_h < 125$ GeV and m_A chosen in the range $145 \text{ GeV} < m_A < 150 \text{ GeV}$, by setting $m_{H^\pm} = m_A$ in order to comply with measurements of Electro-Weak Precision Observables (EWPOs). We finally choose m_A and m_h so that the Z^* boson remains off-shell, i.e., $m_A - m_h < m_Z$.

Regarding the (cosine of the) mixing angle $\cos(\beta - \alpha)$, since we are working within the

IH scenario, this is required to be very close to 1 [4–6]. In our study, for simplicity, we have fixed $\cos(\beta - \alpha) = 1$ exactly. Furthermore, to ensure both theoretical consistency and compatibility with experimental constraints, we have considered values of the ratio of the 2HDM Vacuum Expectation Values (VEVs) in the range $2.5 < \tan\beta < 10$.

By doing so, we have fixed all the free parameters of the CP conserving 2HDM that we assume here, wherein only soft breaking of the discussed \mathbb{Z}_2 symmetry is allowed, as opposed to a hard breaking of it (i.e., $m_{12} \neq 0$ and $\lambda_{6,7} = 0$ in the 2HDM Lagrangian [1]).

A. The DY and $t\bar{t}$ Backgrounds

The DY process and top-(anti)quark pair production and decay are critical backgrounds in numerous analyses at the LHC, particularly in searches for new physics. Sample Feynman diagrams are shown in Figs. 1–2, respectively. The first process occurs when a light quark and antiquark from the protons annihilate, producing a virtual photon or Z boson, which then decay into a pair of leptons ($\ell^+\ell^-$) and initial state radiation fakes the $b\bar{b}$ system. The second one is primarily induced by gluon-gluon fusion (with only a subleading component from $q\bar{q}$ annihilation), where a top quark t and its antiparticle \bar{t} are created together and then decay via $t\bar{t} \rightarrow W^+W^-b\bar{b} \rightarrow \ell^+\ell^-b\bar{b}$ plus missing transverse energy/momentum.

Both processes can be generated at different orders in perturbation theory: i.e., at Leading Order (LO) or in presence of higher order corrections where Quantum Chromo-Dynamics (QCD) and/or EW radiative effects are introduced. The ATLAS and CMS collaborations have carried out comprehensive studies of these two processes across two center-of-mass energies of the LHC, i.e., using the 8 and 13 TeV datasets, for varying values of integrated luminosity (see, e.g., [11], [12] and [13]).

As already mentioned, we have finally used Ref. [3] to calibrate our Monte Carlo (MC) simulation of the two dominant background processes.

B. Parameter Space Sampling, Event Generation and Mass Reconstruction

We selected two BPs for simulating our signal $pp \rightarrow A \rightarrow Zh^* \rightarrow \ell^+\ell^-b\bar{b}$, hereafter, labelled as BP1 and BP2. They have been tested and found to be consistent with current theoretical and experimental constraints, by using HiggsTools [14]. Fla-

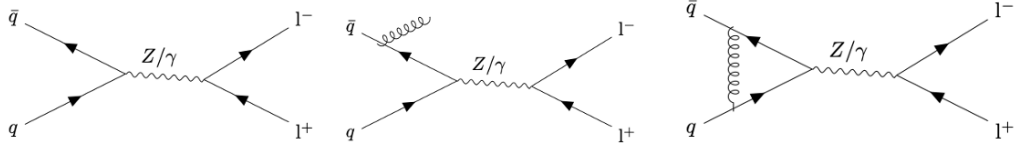


FIG. 1: Representative Feynman diagrams for DY production at LO and in presence of QCD radiation.

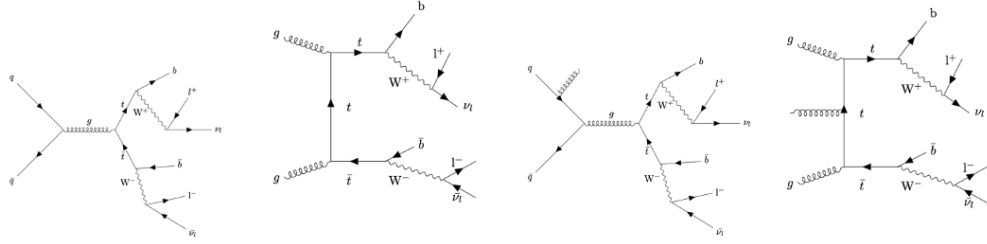


FIG. 2: Representative Feynman diagrams for $t\bar{t}$ production at LO and in presence of QCD radiation.

vor constraints were checked using SuperISO [15]. For BP1, we use $m_A = m_{H^\pm} = 150$ GeV, $m_H = 125$ GeV, $m_h = 68$ GeV, $\tan \beta = 3.9$ whereas for BP2 we use $m_A = m_{H^\pm} = 145$ GeV, $m_H = 125$ GeV, $m_h = 75$ GeV, $\tan \beta = 4$. The mass difference relevant in each case is $m_A - m_h = 82$ GeV in BP1 and 70 GeV in BP2, thus precluding an on-shell Z boson.

We followed the same methodology employed by the CMS collaboration [3] to generate the DY and $t\bar{t}$ backgrounds. That is, the corresponding events were generated at Next-to-LO (NLO) using MadGraph5aMC@NLO [16] with the FxFx merging scheme [17]. The latter enables consistent merging of multi-jet NLO samples and avoids double counting between matrix elements and parton shower emissions. MadSpin was then used to decay the W^\pm and $Z^{(*)}$ bosons to di-leptons. The events were then passed to PYTHIA [18] for parton showering and hadronization, employing the NNPDF 3.0 Parton Distribution Function (PDF) set [19] with the (dynamical) factorization/renormalization scale set by MadGraph5aMC@NLO. Then for all processes we applied detector simulation via Delphes [20] with a standard CMS card [21]. We have then used the same tools and settings for our signal emulation, including the jet merging feature.

Selection cuts were applied on the transverse momentum (p_T), rapidity (η) and separation (ΔR) of (some of) the final-state particles as well as the di-lepton ($m_{\ell^+\ell^-}$) and di-jet ($m_{b\bar{b}}$) invariant masses. We used MadAnalysis5 [22] to manipulate the final state objects, two b -jets and electron/muon pairs. Events with same flavor leptons ($e^\pm e^\mp, \mu^\pm \mu^\mp$) are allowed in the signal definition whereas different flavour leptons ($e^\pm \mu^\mp$) are not. Moreover, for jets, we have applied jet reconstruction by using the anti- k_T algorithm with a cone parameter of 0.4, as implemented in the FastJet package [23].

III. RESULTS

The cuts used initially, based on Ref. [3], were as follows:

- $p_T^{e^\pm} > 25$ GeV (leading), 15 GeV (subleading) and $|\eta(e^\pm)| < 2.5$;
- $p_T^{\mu^\pm} > 20$ GeV (leading), 10 GeV (subleading), and $|\eta(\mu^\pm)| < 2.4$;
- $p_T^{e^\pm \mu^\mp} > 25$ GeV (leading), 15 GeV (subleading e^\pm), 10 GeV (subleading μ^\pm);
- $p_T^j > 20$ GeV and $|\eta(j)| < 2.4$;
- $\Delta R_{jj} > 0.4$ and $\Delta R_{\ell^+\ell^-} > 0.3$;
- $70 \text{ GeV} < m_{\ell^+\ell^-} < 110 \text{ GeV}$.

First, we investigated the significance of the signal for the two BPs with the CMS standard cuts as listed above. As intimated, we have included only the two dominant backgrounds, which are the DY and $t\bar{t}$ processes. In Fig. 3 the mass distribution $m_{\ell^+\ell^-b\bar{b}}$ is analysed using a mass binning width of 28 GeV, as in [3]. This allows us to search for potential excesses of events for each signal BP and to assess the shape of the signal in comparison to the DY and $t\bar{t}$ backgrounds. A similar plot has been shown in the CMS search in [3], but with different signal BPs. Our results for the background processes (lower plot in Fig. 3) agree very well with the corresponding plot in [3], with the peak at around 200 GeV for DY and at around 250 GeV for $t\bar{t}$. For the two signal BPs one sees that the peak in $m_{\ell^+\ell^-b\bar{b}}$ is at the mass of m_A , as expected, but the number of signal events is much less than that of the background. Hence there would be no possibility of observing a statistical significant signal in our case, where the primary decay is $A \rightarrow Z^*h$. We in fact note that the cut $70 \text{ GeV} < m_{\ell^+\ell^-} < 110$

GeV was employed by CMS in [3] in order to keep most of the signal events in the decay $H \rightarrow ZA$ with a real Z . However, this cut removed a large fraction of the signal events for our BPs with an off-shell Z^* , as the $m_{\ell+\ell-}$ distribution from Z^* would not be expected to concentrate in the region $70 \text{ GeV} < m_{\ell+\ell-} < 110 \text{ GeV}$ (for our BPs).

In order to probe the case of off-shell Z^* (for which no limits are set in [3] or elsewhere), it was necessary to change the $70 \text{ GeV} < m_{\ell+\ell-} < 110 \text{ GeV}$ cut such that more of the signal events are retained. Such a modification also has favorable consequences for the magnitude of the background, as we will see below. In order to find an optimum $m_{\ell+\ell-}$ cut we analyzed the mass distributions $m_{\ell+\ell-}$ and $m_{b\bar{b}}$ for the DY and $t\bar{t}$ backgrounds and compared these with those of the signal. At this stage, no cuts were applied on $m_{\ell+\ell-}$ or $m_{b\bar{b}}$ but all other selection cuts were kept (i.e., p_T , η etc.). For the backgrounds, in Fig. 4, one can see that the peak of the DY process is at $m_{\ell+\ell-} = m_Z$, as expected (as the process involves a decaying on-shell Z), while the peak of the $t\bar{t}$ background (in which the leptons originate from W^\pm bosons) is at a lower value than m_Z . For the $m_{b\bar{b}}$ distribution in the backgrounds, the peak is at around 100 GeV for both processes, although the $b\bar{b}$ pairs have a different origin in DY and $t\bar{t}$, being from Initial State Radiation (ISR) mistagged gluons (primarily) in the former case and from actual b -jets from $t\bar{t}$ decays in the latter case. Fig. 5 for the signal illustrates that the peak in $m_{\ell+\ell-}$ is indeed not at m_Z : BP1 (which has a less off-shell Z^* due to the larger value of $m_A - m_h$) having its peak at a larger value of $m_{\ell+\ell-}$ than BP2. In the distribution in $m_{b\bar{b}}$ ones sees that the peak corresponds to the mass of m_H (as expected, because $H \rightarrow b\bar{b}$).

Given the differences in the $m_{\ell+\ell-}$ and $m_{b\bar{b}}$ distributions for the signal and backgrounds, in order to enhance the significance of the former over the latter, we choose the cuts $20 \text{ GeV} < m_{\ell+\ell-} < 50 \text{ GeV}$ and $m_{b\bar{b}} < 100 \text{ GeV}$, with the $m_{\ell+\ell-}$ cut causing the greater suppression of the background. These requirements were chosen based on the expected kinematic features of the signal, specifically, the presence of an off-shell Z^* boson and a light Higgs boson (i.e., h with a mass below 125 GeV). These particular values were selected to significantly reduce the dominant background contributions while retaining a significant portion of the signal. However, no formal optimization (such as a parameter scan or significance maximization) was carried out. As such, the cuts used in this study are illustrative rather than final.

In Fig. 6 we display the signals and backgrounds as a function of the four-body invariant mass distribution $m_{\ell+\ell-b\bar{b}}$ with the above cuts on $m_{\ell+\ell-}$ and $m_{b\bar{b}}$ being applied. One can see

Scenario	S	S	B	\mathcal{S}_1	\mathcal{S}_1	\mathcal{S}_2	\mathcal{S}_2
	BP1	BP2		BP1	BP2	BP1	BP2
$70 \text{ GeV} < m_{\ell^+\ell^-} < 110 \text{ GeV}$	178	116	13924	1.5	0.9	1.4	0.86
$20 \text{ GeV} < m_{\ell^+\ell^-} < 50 \text{ GeV}$ and $m_{b\bar{b}} < 100 \text{ GeV}$	153	100	9	43	28	12	9.5

TABLE I: Signal (S), background (B) and significances (\mathcal{S}_1 and \mathcal{S}_2) for two BPs where $20 \text{ GeV} < m_{\ell^+\ell^-b\bar{b}} < 180 \text{ GeV}$ with an integrated luminosity of 35.9 fb^{-1} .

that the signals are now very prominent above a much smaller background, thus allowing the case of the $A \rightarrow HZ^*$ signal to be probed. We remind the reader here that the case with Z^* currently has no limits set on the (m_A, m_H) plane from the CMS search in [3].

In the remainder of our analysis, we evaluate the statistical significance of the signals over the backgrounds using two common definitions of it. The first definition is $\mathcal{S}_1 = S/\sqrt{B}$, where S is the number of signal events and B is the number of background events. The second definition is $\mathcal{S}_2 = S/\sqrt{S+B}$, which accounts for statistical fluctuations in both signal and background. Both results are reported in Tab. I, for the luminosity 35.9 fb^{-1} . The latter makes two key points. On the one hand, if the CMS search of [3] were applied as is to our proposed signal, it would have no sensitivity to it. On the other hand, if modified suitably as recommended here, such a search would afford one with dramatic discovery possibilities. In all generality, based on previous work of ours on the size of the signal $pp \rightarrow A \rightarrow Z^*h \rightarrow \ell^+\ell^-b\bar{b}$ in the 2HDM Type-I in IH [4–6], we conclude that such a level of sensitivity would exist over a sizable region of its parameters space.

IV. CONCLUSIONS

In this paper, we have demonstrated that optimized selection criteria can significantly enhance the LHC observability of the signal process $pp \rightarrow A \rightarrow Z^*h \rightarrow \ell^+\ell^-b\bar{b}$ within the framework of the 2HDM Type-I, specifically, under the assumption of an IH wherein $m_h < m_H = 125 \text{ GeV}$. In particular, by investigating mass selection cuts alternative to the CMS baseline used in Higgs searches in the $\ell^+\ell^-b\bar{b}$ final state (wherein an on-shell Z boson is sought), specifically, targeting the low $m_{\ell^+\ell^-}$ region and imposing an upper bound on $m_{b\bar{b}}$, we have shown that dominant backgrounds from the DY and $t\bar{t}$ processes

can be substantially reduced. This ultimately leads to a notable improvement in the signal significance of the target signal process, whichever its definition. Our results highlight the effectiveness of the refined kinematic selections and we thus encourage the LHC collaborations to carry out a search for $pp \rightarrow A \rightarrow Z^* h \rightarrow \ell^+ \ell^- b \bar{b}$ along the lines presented here, with the aim of increasing sensitivity to the regions of the (m_A, m_h) plane where $m_A - m_h < m_Z$, i.e., the Z^* is off shell, a kinematic configuration not presently considered experimentally.

Acknowledgements

SA acknowledges the use of the IRIDIS High Performance Computing Facility and associated support services at the University of Southampton. SA further acknowledges support from a scholarship of the Imam Mohammad Ibn Saud Islamic University. AA and SM are funded in part by the STFC CG ST/X000583/1 and SM also through the NExT Institute.

-
- [1] G. C. Branco, P. M. Ferreira, L. Lavoura, M. N. Rebelo, M. Sher and J. P. Silva, “Theory and phenomenology of two-Higgs-doublet models,” *Phys. Rept.* **516**, 1–102 (2012) doi:10.1016/j.physrep.2012.02.002 [arXiv:1106.0034 [hep-ph]].
 - [2] S. Senglali, H. Day-Hall, S. Moretti and R. Benbrik, “Mapping $pp \rightarrow A \rightarrow ZH \rightarrow l^+ l^- b \bar{b}$ and $pp \rightarrow H \rightarrow ZA \rightarrow l^+ l^- b \bar{b}$ current and future searches onto 2HDM parameter spaces,” *Phys. Lett. B* **810**, 135819 (2020) doi:10.1016/j.physletb.2020.135819 [arXiv:2006.05177 [hep-ph]].
 - [3] A. M. Sirunyan *et al.* [CMS Collaboration], “Search for new neutral Higgs bosons through the $H \rightarrow ZA \rightarrow \ell^+ \ell^- b \bar{b}$ process in pp collisions at $\sqrt{s} = 13$ TeV,” *JHEP* **03**, 055 (2020) doi:10.1007/JHEP03(2020)055 [arXiv:1911.03781 [hep-ex]].
 - [4] A. G. Akeroyd, S. Alanazi and S. Moretti, “The decay $A^0 \rightarrow h^0 Z^*$ in the inverted hierarchy scenario and its detection prospects at the LHC,” *J. Phys. G* **50**, no.9, 095001 (2023) doi:10.1088/1361-6471/ace3e1 [arXiv:2301.00728 [hep-ph]].
 - [5] A. G. Akeroyd, S. Alanazi and S. Moretti, “The process $gg \rightarrow h^0 Z^*$ in the inverted hierarchy scenario of the 2HDM type-I at the LHC,” *Eur. Phys. J. C* **84**, no.11, 1172 (2024) doi:10.1140/epjc/s10052-024-13548-1 [arXiv:2405.18990 [hep-ph]].

- [6] A. G. Akeroyd, S. Alanazi and S. Moretti, “Probing the decay $A^0 \rightarrow h^0 Z^{(*)}$ in Two-Higgs-Doublet Models in the inverted hierarchy scenario at the LHC,” [arXiv:2408.08314 [hep-ph]].
- [7] E. Accomando, M. Chapman, A. Maury and S. Moretti, “Below-threshold CP-odd Higgs boson search via $A \rightarrow Z^* h$ at the LHC,” Phys. Lett. B **818**, 136342 (2021) doi:10.1016/j.physletb.2021.136342 [arXiv:2002.07038 [hep-ph]].
- [8] A. M. Sirunyan *et al.* [CMS Collaboration], “Search for a heavy pseudoscalar boson decaying to a Z and a Higgs boson at $\sqrt{s} = 13$ TeV,” Eur. Phys. J. C **79**, no.7, 564 (2019) doi:10.1140/epjc/s10052-019-7058-x [arXiv:1903.00941 [hep-ex]].
- [9] [ATLAS Collaboration], “Search for Higgs boson decays $A \rightarrow Zh$ in pp collisions at $\sqrt{s} = 8$ TeV with the ATLAS detector,” Phys. Lett. B **744**, 163–183 (2015) doi:10.1016/j.physletb.2015.03.054.
- [10] [ATLAS Collaboration], “Search for a heavy Higgs boson decaying into a Z boson and another heavy Higgs boson in the $\ell\ell b\bar{b}$ and $\ell\ell WW$ final states in pp collisions at $\sqrt{s} = 13$ TeV with the ATLAS detector,” Eur. Phys. J. C **81**, no.5, 396 (2021) doi:10.1140/epjc/s10052-021-09117-5 [arXiv:2102.11582 [hep-ex]].
- [11] ATLAS Collaboration, “Measurement of the transverse momentum distribution of Drell-Yan lepton pairs in proton-proton collisions at $\sqrt{s} = 13$ TeV with the ATLAS detector,” arXiv:1912.02844 [hep-ex] (2020). URL: <https://arxiv.org/abs/1912.02844>.
- [12] ATLAS Collaboration, “Measurement of double-differential charged-current Drell-Yan cross-sections at high transverse masses in pp collisions at $\sqrt{s} = 13$ TeV with the ATLAS detector,” JHEP 07 (2025) 026. DOI: 10.1007/JHEP07(2025)026.
- [13] CMS Collaboration, “First measurement of the top quark pair production cross section in proton-proton collisions at $\sqrt{s} = 13.6$ TeV,” JHEP 08 (2023) 204. DOI: 10.1007/JHEP08(2023)204.
- [14] H. Bahl, T. Biekötter, S. Heinemeyer, C. Li, S. Paasch, G. Weiglein, J. Wittbrodt, “HiggsTools: BSM scalar phenomenology with new versions of HiggsBounds and HiggsSignals,” Comput. Phys. Commun. 291 (2023) 108803. DOI: 10.1016/j.cpc.2023.108803.
- [15] F. Mahmoudi, “SuperIso v2.3: A Program for calculating flavor physics observables in Supersymmetry,” Comput. Phys. Commun. 180 (2009) 1579–1613. DOI: 10.1016/j.cpc.2009.02.017. arXiv:0808.3144 [hep-ph].
- [16] J. Alwall, R. Frederix, S. Frixione, V. Hirschi, F. Maltoni, O. Mattelaer, H.S. Shao, T. Stelzer,

- P. Torrielli, M. Zaro, “The automated computation of tree-level and next-to-leading order differential cross sections, and their matching to parton shower simulations,” *JHEP* 07 (2014) 079. DOI: 10.1007/JHEP07(2014)079. arXiv:1405.0301 [hep-ph].
- [17] R. Frederix, S. Frixione, “Merging meets matching in MC@NLO,” *JHEP* 12 (2012) 061. DOI: 10.1007/jhep12(2012)061.
- [18] T. Sjöstrand, S. Ask, J.R. Christiansen, R. Corke, N. Desai, P. Ilten, S. Mrenna, S. Prestel, C.O. Rasmussen, P. Skands, “An Introduction to PYTHIA 8.2,” *Comput. Phys. Commun.* 191 (2015) 159–177. DOI: 10.1016/j.cpc.2015.01.024. arXiv:1410.3012 [hep-ph].
- [19] R. D. Ball *et al.* [NNPDF], “Parton distributions for the LHC Run II,” *JHEP* **04**, 040 (2015), arXiv:1410.8849 [hep-ph].
- [20] J. de Favereau, C. Delaere, P. Demin, A. Giammanco, V. Lemaître, A. Mertens and M. Selvaggi, “DELPHES 3: A modular framework for fast simulation of a generic collider experiment,” *JHEP* **02**, 057 (2014), doi:10.1007/JHEP02(2014)057, arXiv:1307.6346 [hep-ex].
- [21] A. Mertens, “New Developments for Fast Detector Simulation in ATLAS,” *J. Phys. Conf. Ser.* **608**, no.1, 012045 (2015), doi:10.1088/1742-6596/608/1/012045.
- [22] E. Conte, B. Fuks and G. Serret, “MadAnalysis 5, A User-Friendly Framework for Collider Phenomenology,” *Comput. Phys. Commun.* **184**, 222-256 (2013), doi:10.1016/j.cpc.2012.09.009, arXiv:1206.1599 [hep-ph].
- [23] M. Cacciari, G. P. Salam and G. Soyez, “FastJet user manual,” *Eur. Phys. J. C* **72**, 1896 (2012), doi:10.1140/epjc/s10052-012-1896-2, arXiv:1111.6097 [hep-ph].

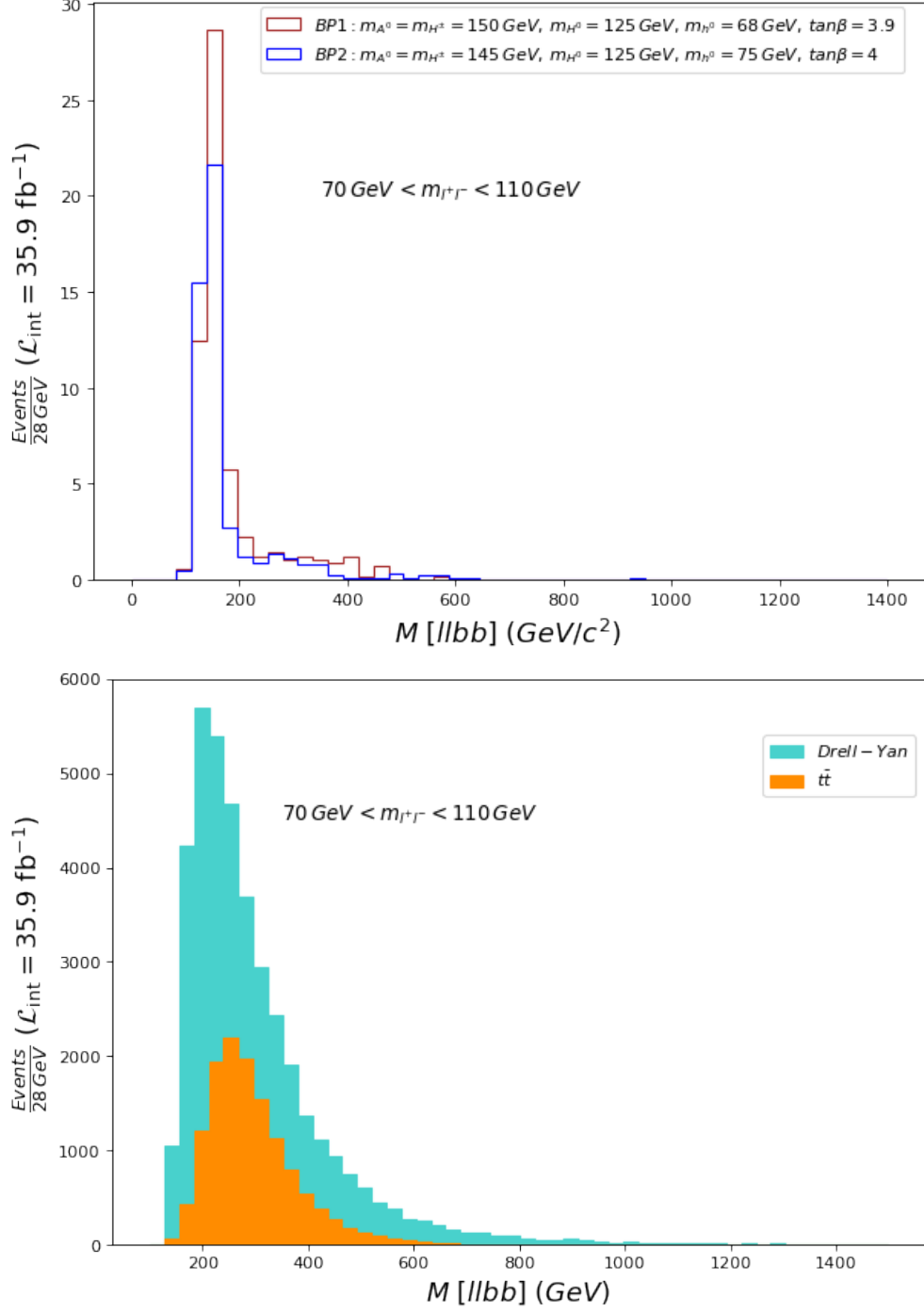


FIG. 3: Signal and the background processes as a function of $m_{\ell^+\ell^-b\bar{b}}$ for $70 \text{ GeV} < m_{\ell^+\ell^-} < 110 \text{ GeV}$.

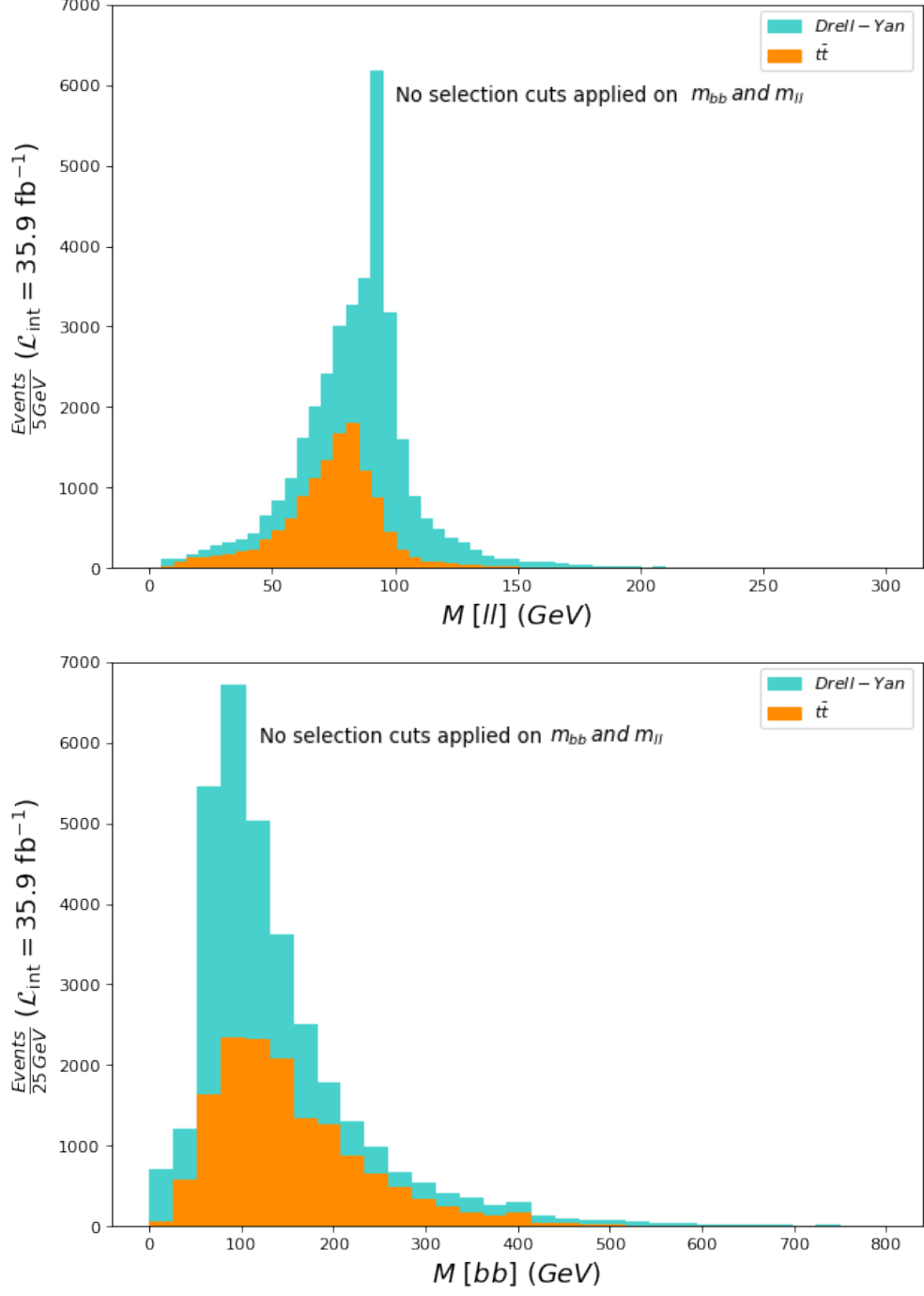


FIG. 4: The background processes as a function of $m_{\ell+\ell-}$ and $m_{b\bar{b}}$ without any cuts applied on $m_{\ell+\ell-}$ or $m_{b\bar{b}}$.

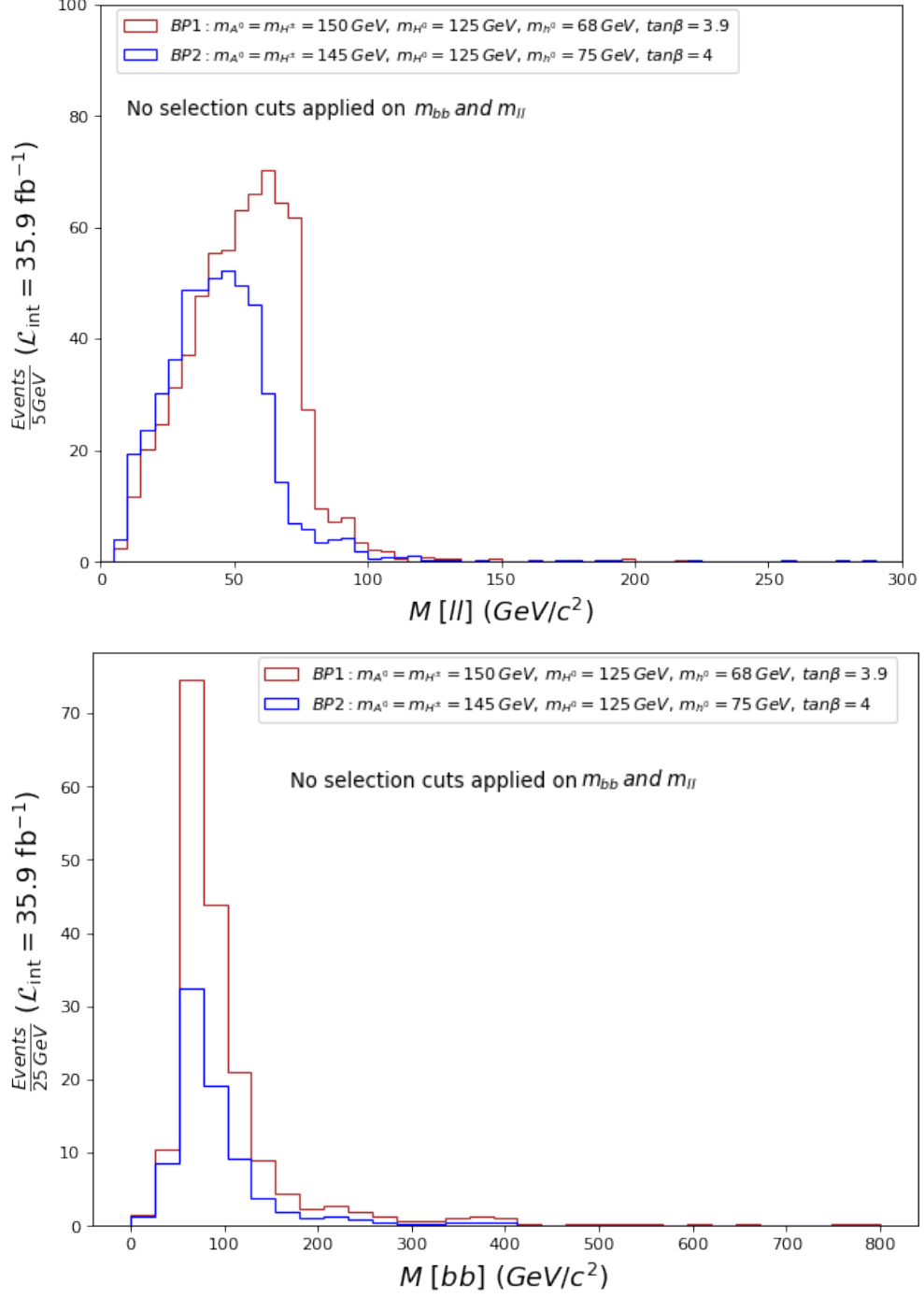


FIG. 5: Signal rates as a function of $m_{\ell^+\ell^-}$ and $m_{b\bar{b}}$ without any cuts applied on $m_{\ell^+\ell^-}$ or $m_{b\bar{b}}$.

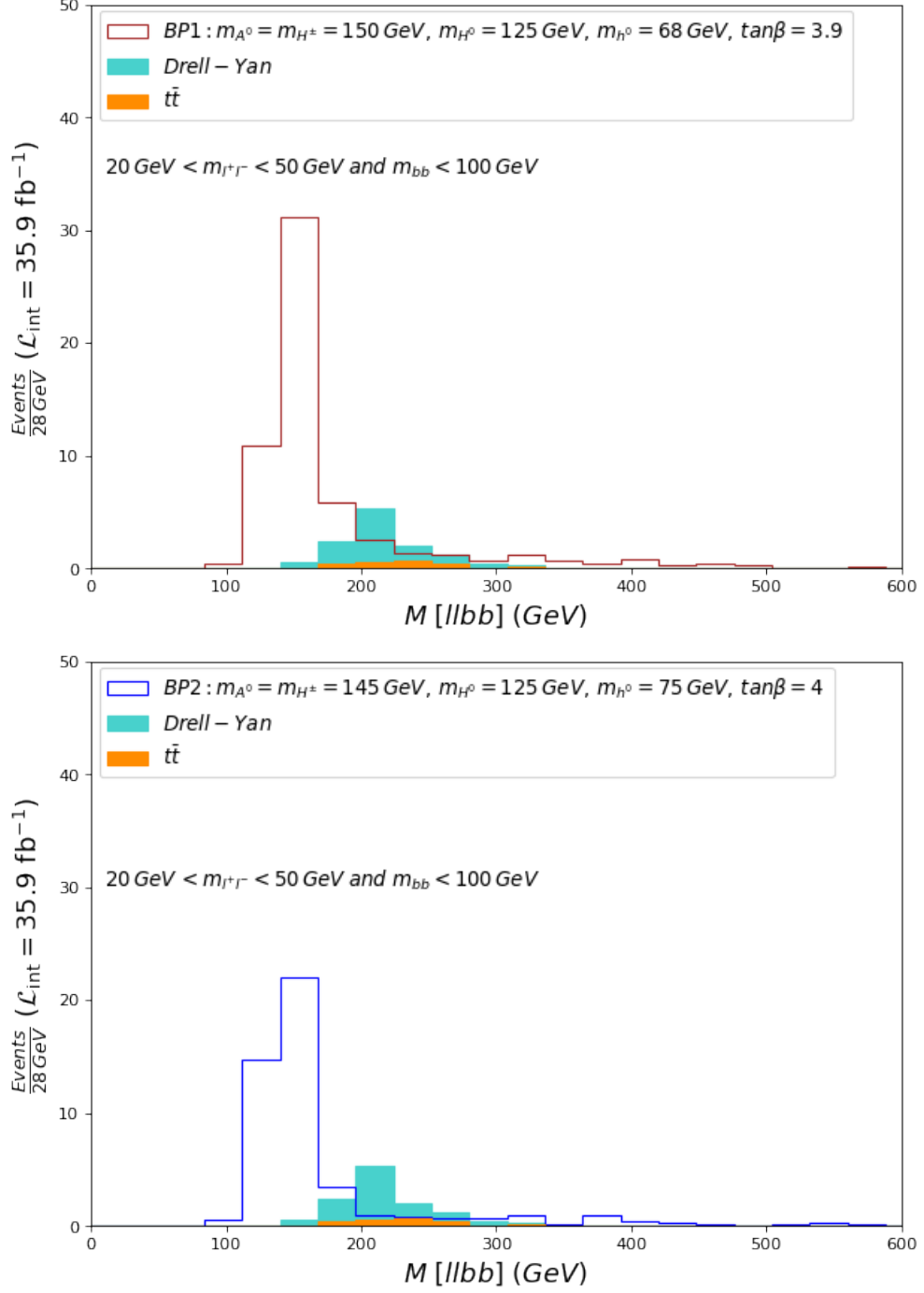


FIG. 6: Signal and background processes as a function of $m_{\ell^+\ell^-\bar{b}\bar{b}}$ for $20 \text{ GeV} < m_{\ell^+\ell^-} < 50 \text{ GeV}$ and $m_{b\bar{b}} < 100 \text{ GeV}$.